ECCOMAS Congress 2016
VII European Congress on Computational Methods in Applied Sciences and Engineering
M. Papadrakakis, V. Papadopoulos, G. Stefanou, V. Plevris (eds.)
Crete Island, Greece, 5–10 June 2016

ECCENTRICALLY BRACED FRAMES DESIGNED FOR THE ENERGY DISSIPATION OPTIMIZATION

Elide Nastri[1]

[1] University of Salerno
Via Giovanni Paolo II, 132, 84084, Fisciano (SA), Italy
e-mail: enastri@unisa.it

Keywords: Eccentrically Braced Frames, dissipation optimization, steel, dissipative devices, free from damage structures, Theory of Plastic Mechanism Control.

Abstract. *The work herein presented has the main purpose to show a practical application of a proper design procedure able to dimension Eccentrically Braced Frames with Inverted Y-scheme equipped with removable dissipative devices substituting the link member. Column bases are conceived with pin-jointed base connections in order to assure that the global mechanism is achieved only when link members results activated in plastic range. The control of devices activation and the optimization of energy dissipation capacity is obtained by applying a rigorous design procedure assuring that only the dissipative zones are involved in plastic range while non dissipative ones remain in elastic range. Dissipative devices are designed in order to bear the whole storey seismic shear without a strength and stiffness degradation. In addition, being the link members substituted by dissipative devices, column bases pin jointed and column sections designed in order to remain in elastic range by a properly design procedure, the structure can be considered as free from damage. In fact after a destructive seismic event all the damaged devices can be replaced by new ones. The accuracy of the design approach has been investigated by means push-over and non-linear dynamic analyses by applying a properly chosen set of earthquake ground motions.*

1 INTRODUCTION

In the framework of seismic resistant structure, Eccentrically Braced Frames (EBFs) constitute a quite recent structural typology. They gained prominence thanks to the study of Popov and Kasai [1]-[3]. This structural typology is well suited for tall buildings located in areas of high seismic intensity. For this reason, EBFs are especially widespread in USA and New Zealand where the recent Christchurch earthquake of the February 11th 2011 put to the test a great number of structures. In particular, this unfortunate event allowed testing on real scale the damage a high intensity earthquake is able to bring on EBF steel frames. As regards their working under seismic actions, EBFs constitute a suitable compromise between seismic resistant MR-frames and concentrically braced frames because they exhibit both adequate lateral stiffness, due to the high contribution coming from the diagonal braces, and ductile behaviour, due to the ability of the links, constituting the dissipative zones of this structural typology, in developing wide and stable hysteresis loops. Therefore, the optimization of dissipative behaviour of this structural typology is obtained when all the links are involved in plastic range. In this paper, reference is made to Inverted Y-scheme EBFs, that are a particular configuration of EBFs reported in Eurocode 8 [4] still not sufficiently investigated and not largely widespread despite having many advantages both in term of performance and construction. Its main characteristic is that the link, i.e. the dissipative zone, does not belong to the beam member. In fact, one of the primary benefits in using such structural typology regards the chance to substitute easily the damaged link after a destructive seismic event, and, in addition, the possibility to conceive the scheme within the framework of supplementary energy dissipation [5]-[10], by substituting the vertical link member with a dissipative device, such as a friction damper [11] or hysteretic damper, which is able to exhibit a highly dissipative behaviour if compared with traditional link members. As damaged links can be easily removed and substituted after earthquake, such structural scheme exhibits the greatest advantages provided that the other structural members as beams, diagonals and columns, have been not damaged during the seismic event, i.e. have remained in elastic range. This is precisely why a proper design is of paramount importance. In fact, only with collapse mechanism of global type it is possible to assure that damage is concentrated only in dissipative zones while the other non-dissipative ones remain in elastic range. This important scope is, out of doubts, the strength of the Theory of Plastic Mechanism Control.

The Theory of Plastic Mechanism Control (TPMC) [12], differently from the rules proposed by EC8 allows designing structure always showing at the collapse a mechanism of global type. This result is assured thanks both to the strong background of the theory, that is based on the kinematic theorem of plastic collapse, than to the successive improvements of the design procedure that have led to a recent version that is easy to be carried out by means of hand calculation. This last form of the design procedure is the so called "closed form solution of TPMC" that has been satisfactorily applied to design both MRFs [13] than EBF-MRFs dual systems [14]. However, this procedure in the previous but as the same efficient form as the improved one has been applied to design all the structural steel typology [15] - [30] and also reinforced concrete MRFs [31]-[32].

Even though, this procedure is able to assure a collapse mechanism of global type, the seismic optimization has to be pursued by assuring that all the dissipative zones engage in yielding as possible as the same time [33]. For this reason, in this structural example, link members, have been substituted by innovative devices [34] inspired to frictional devices investigated in the framework of the European Research Project "FREEDAM". As a consequence the design procedure based on TPMC has improved to promote the contemporary activation of all dissipative devices by additionally considering the column bases at the first storey, beam and diagonal ends has simply pinned. In this way, being only the device activated, beams, diagonals and column bases pin jointed and column sections designed in order to remain in elastic range by a properly design procedure, the structure can be considered as free from damage [11], [35]. The accuracy of the design approach has been investigated by means push-over and non-linear dynamic analyses by applying a properly chosen set of earthquake ground motions.

2 DESIGN APPROACH

The "Theory of Plastic Mechanism Control" design approach has the aim to provide structures able to fail with a collapse mechanism of global type. Global mechanism represents the optimum in term of structural dissipation capacity being all the dissipative zones involved in the pattern of yielding while the non dissipative ones remain in elastic range. Dissipative zones of traditional EBFs are the links and the bases of the column at the first storey. However, in this particular case, links are substituted by special dissipative devices and column bases at the bottom of the first storey by means of pin connections. In this way plastic hinges cannot develop at the bottom of the first storey columns, so that, only the link ends are involved in plastic range being beam equally hinged at their ends. In order to design members to fulfil this design goal devices and column sections have to be designed in order to assure on one hand the optimization of the seismic response and from the other hand a collapse mechanism of global type. The first design unknown having to be provided are the devices substituting link members for which, the whole sum of design slip moment has to be provided by assuring that, according with the kinematic theorem of plastic collapse extended to the concept of mechanism equilibrium curve, the collapse multiplier α of the seismic storey forces F_k has to be at least equal to 1 at a design displacement δ_u compatible with the ductility supply of dissipative zone:

$$\alpha = \alpha_0^{(g)} - \gamma^{(g)}\delta_u \geq 1 \;\; \Rightarrow \;\; \frac{2M_{fl.Ed.n_s}\sum_{k=1}^{n_s}\beta_k}{\sum_{k=1}^{n_s}F_k h_k} - \gamma^{(g)}\delta_u \geq 1 \tag{1}$$

where $\alpha_0^{(g)}$is the first order collapse multiplier:

$$\alpha_0^{(g)} = \frac{2M_{fl.Ed.n_s}\sum_{k=1}^{n_s}\beta_k}{\sum_{k=1}^{n_s}F_k h_k} \tag{2}$$

and $\gamma^{(g)}$ is the slope of mechanism equilibrium curve accounting for second order effects:

$$\gamma^{(g)} = \frac{\frac{1}{h_{ns}}\sum_{k=1}^{n_s}V_k h_k}{\sum_{k=1}^{n_s}F_k h_k} \tag{3}$$

In particular, V_k and h_k are the sum of all the vertical loads acting at each storey and the storey height, respectively. By designing dissipative zones proportionally to the storey shear they are assured to be engaged in yielding as contemporary as possible, benefit optimization of the seismic response. In addition, the design ultimate displacement has to be dependent on the device stroke, i.e. the ultimate distance the dissipative device is able to tread by slippage. By solving as an equality Eq. (1) it is possible to provide the sum of design slip moments of devices at the last storey , $M_{fl.Ed.n_s}$:

$$M_{fl.Ed.n_s}\sum_{k=1}^{n_s}\beta_k = \frac{\left(\gamma^{(g)}\delta_u + 1\right)}{2}\sum_{k=1}^{n_s}F_k h_k \tag{4}$$

that shared by the term $\beta_k = \sum_{i_m=k}^{n_s}F_k / F_{n_s}$, [36]-[37] provides the sum of design slip moment at each storey optimized to promote the contemporary engagement in slippage, $M_{fl.Ed.k}$:

$$M_{fl.Ed.k} = \beta_k M_{fl.Ed.n_s} \tag{5}$$

In addition, if the same frame has more braced bays the quantity provided by Eq. (5) need to be shared between all the devices belonging to the braced bay.

The design slip moment $M_{fl.Ed.jk}$ is used to design frictional devices whose resistance is expressed by means of the following term $M_{fl.Cd.jk}$.

Beams are non dissipative zones and to be designed by means as the maximum among the design moment belonging to the vertical load distribution and, according to the second capacity design principle, those provided by a local hierarchy criterion where γ_{Rd} is an overstrength factor [26].

$$M_{b.Cd.jk} = \max\left(\frac{q_{v.j}L_j^2}{8}; \gamma_{Rd}\frac{M_{fl.Cd.jk}}{2}\right) \tag{6}$$

As regards the column design, all the possible mechanism typology which can affect a seismic resistant frame should be considered. In particular, it is possible to observe that EBFs under seismic horizontal forces should fail according to three main collapse typologies called type-1, type-2 and type-3, as reported in Figure 1 for the specific case of pin-jointed column bases where the rectangles represents the dissipative devices involved while the solid circles the plastic hinges developing at the top or bottom end of columns for undesired mechanisms. Every one of these can involve each storey and, for this reason, being the number of storey equal to n_s the number of possible mechanisms involving a structure can be easily computed as $3n_s$. Only one of these mechanisms is the desired one, i.e. the global one, and it is a particular case of type-2 mechanism extended to all the n_s storeys. It means that all the other $3n_s - 1$ mechanisms are undesired and must be avoid by applying TPMC.

The design conditions also found their theoretical bases in the kinematic theorem of plastic collapse extended to the concept of collapse mechanism equilibrium curve which is representative of a straight line whose intercept with the vertical axis in a Cartesian diagram is the collapse mechanism multiplier of the first order, $\alpha_{i_m}^{(t)}$, while $\gamma_{i_m}^{(t)}$is the slope where i_m and t are the mechanism index and the mechanism typology code respectively.

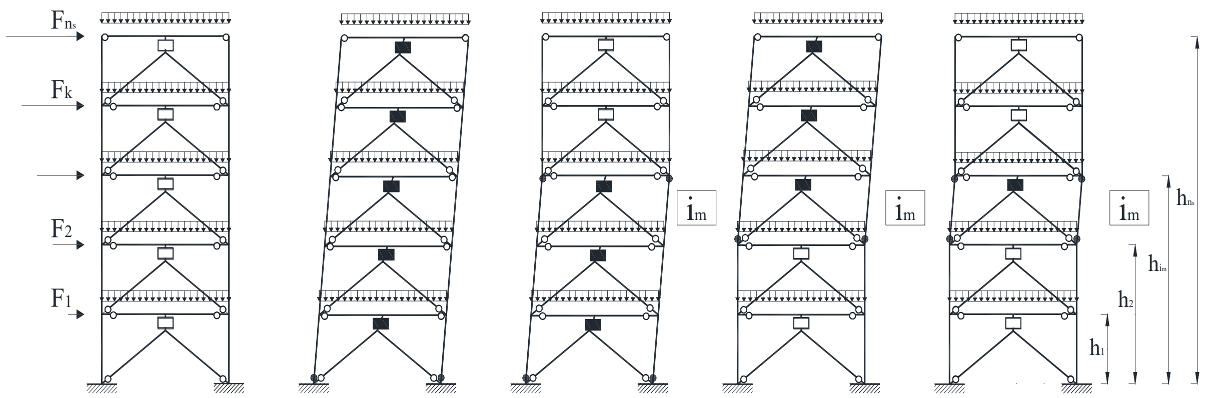

Figure 1: Collapse mechanism of Inverted Y EBFs equipped with dissipative devices

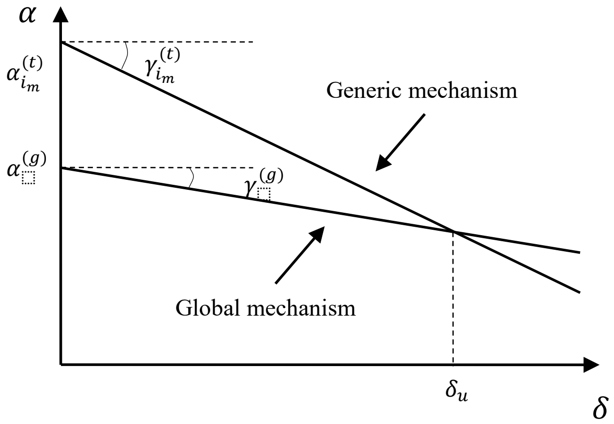

Figure 2: Design condition for the failure mode control

TPMC states that the global mechanism equilibrium curve has to be located below those corresponding to all the other mechanisms within a displacement range compatible with the plastic deformation capacity of dissipative zones, δ_u (Figure 2). Consequently, the design conditions are provided by the following equations:

$$\alpha^{(g)} - \gamma^{(g)}\delta_u \le \alpha_{i_m}^{(t)} - \gamma_{i_m}^{(t)}\delta_u \qquad i_m = 1,2,3,\dots,n_s \qquad t = 1,2,3 \tag{7}$$

The computation of the quantities $\alpha_{i_m}^{(t)}$ and $\gamma_{i_m}^{(t)}$ exploits the virtual work principle and it is amply detailed and discussed in a previous work [5]-[13]. In particular, the expressions of $\alpha_{i_m}^{(t)}$ and $\gamma_{i_m}^{(t)}$ are reported in Table 1. In particular, according to the second capacity design principle, non dissipative zones have to be designed according to the maximum actions that dissipative zones, i.e. dissipative devices, are able to transmit in their ultimate conditions. For this reason, frictional device overstrength have to be considered by introducing the over-strength factor γ_{Rd}.

Type-1	***Type-2***	***Type-3***
$\alpha_{0.i_m}^{(1)} = \dfrac{\gamma_{Rd} 2M_{fl.Cd.n_s}\sum_{k=1}^{i_m-1}\beta_k + \sum_{i=1}^{n_c} M_{c.ii_m}^{(1)}}{\sum_{k=1}^{i_m} F_k h_k + h_{i_m}\sum_{k=i_m+1}^{n_s} F_k}$	$\alpha_{0.i_m}^{(2)} = \dfrac{\sum_{i=1}^{n_c} M_{c.ii_m}^{(2)} + \gamma_{Rd} 2M_{fl.Cd.n_s}\sum_{k=i_m}^{n_s}\beta_k}{\sum_{k=i_m}^{n_s} F_k (h_k - h_{i_m-1})}$	$\alpha_{0.i_m}^{(3)} = \dfrac{2\sum_{i=1}^{n_c} M_{c.ii_m}^{(3)}}{(h_{i_m} - h_{i_m-1})\sum_{k=i_m}^{n_s} F_k}$
$\gamma_{i_m}^{(1)} = \dfrac{\sum_{k=1}^{i_m} V_k h_k + h_{i_m}\sum_{k=i_m+1}^{n_s} V_k}{h_{i_m}\left(\sum_{k=1}^{i_m} F_k h_k + h_{i_m}\sum_{k=i_m+1}^{n_s} F_k\right)}$	$\gamma_{i_m}^{(2)} = \dfrac{\sum_{k=i_m}^{n_s} V_k (h_k - h_{i_m-1})}{(h_{n_s} - h_{i_m-1})\sum_{k=i_m}^{n_s} F_k (h_k - h_{i_m-1})}$	$\gamma_{i_m}^{(3)} = \dfrac{\sum_{k=i_m}^{n_s} V_k}{(h_{i_m} - h_{i_m-1})\sum_{k=i_m}^{n_s} F_k}$

Table 1. First order and second order collapse mechanism multiplier at the generic $i_m -$ th storey

Therfore, by substituting terms reported in Table 1 in Eq. (7), the following design relationship are obtained for type-1 mechanism:

$$\gamma_{Rd}\frac{2M_{fl.Cd.n_s}\sum_{k=1}^{n_s}\beta_k}{\sum_{k=1}^{n_s} F_k h_k} - \gamma^{(g)}\delta_u \le \frac{2M_{fl.Cd.n_s}\sum_{k=1}^{i_m-1}\beta_k + \sum_{i=1}^{n_c} M_{c.ii_m}^{(1)}}{\sum_{k=1}^{i_m} F_k h_k + h_{i_m}\sum_{k=i_m+1}^{n_s} F_k} - \gamma_{i_m}^{(1)}\delta_u \tag{8}$$

for type-2 mechanism:

$$\gamma_{Rd}\frac{2M_{fl.Cd.n_s}\sum_{k=1}^{n_s}\beta_k}{\sum_{k=1}^{n_s} F_k h_k} - \gamma^{(g)}\delta_u \le \frac{\sum_{i=1}^{n_c} M_{c.ii_m}^{(2)} + \gamma_{Rd} 2M_{fl.Cd.n_s}\sum_{k=i_m}^{n_s}\beta_k}{\sum_{k=i_m}^{n_s} F_k (h_k - h_{i_m-1})} - \gamma_{i_m}^{(2)}\delta_u \tag{9}$$

and for type-3 mechanism :

$$\begin{aligned} &for\ i_m = 1 \qquad \gamma_{Rd}\frac{2M_{fl.Cd.n_s}\sum_{k=1}^{n_s}\beta_k}{\sum_{k=1}^{n_s}F_k h_k} - \gamma^{(g)}\delta_u \le \frac{\sum_{i=1}^{n_c}M_{c.i1}^{(3)}}{h_1\sum_{k=1}^{n_s}F_k} - \gamma_1^{(3)}\delta_u \\ &for\ i_m > 1 \qquad \gamma_{Rd}\frac{2M_{fl.Cd.n_s}\sum_{k=1}^{n_s}\beta_k}{\sum_{k=1}^{n_s}F_k h_k} - \gamma^{(g)}\delta_u \le \frac{2\sum_{i=1}^{n_c}M_{c.ii_m}^{(3)}}{\left(h_{i_m} - h_{i_m-1}\right)\sum_{k=i_m}^{n_s}F_k} - \gamma_{i_m}^{(3)}\delta_u \end{aligned} \tag{10}$$

That rearranged to provide the unknown of the design procedure, i.e. the sum of column plastic moment at each storey $M_{c.ii_m}^{(t)}$ reported in the following.

In particular, at the first storey the condition reported in Eq. (8) provide only one design relationship being easily demonstrable that mechanism type-1 and type-3 at the first storey are coincident and mechanism type-2 is coincident with the global one:

$$\sum_{i=1}^{n_c} M_{c.i1}^{(1or3)} \ge \left[\gamma_{Rd}\frac{2M_{fl.Ed.n_s}\sum_{k=1}^{n_s}\beta_k}{\sum_{k=1}^{n_s}F_k h_k} + \left(\gamma_1^{(3)} - \gamma^{(g)}\right)\delta_u\right]\left(h_{i_m} - h_{i_m-1}\right)\sum_{k=i_m}^{n_s}F_k \tag{11}$$

At the $i_m > 1$ storeys, design conditions have to be make explicit for all the undesired mechanism typologies:

$$\begin{aligned} \sum_{i=1}^{n_c} M_{c.ii_m}^{(1)} \ge & \left[\gamma_{Rd}2M_{fl.Cd.n_s}\left(\frac{\sum_{k=1}^{n_s}\beta_k}{\sum_{k=1}^{n_s}F_k h_k} - \frac{\sum_{k=1}^{i_m-1}\beta_k}{\sum_{k=1}^{i_m}F_k h_k + h_{i_m}\sum_{k=i_m+1}^{n_s}F_k}\right)\right. \\ & \left. + \left(\gamma_{i_m}^{(1)} - \gamma^{(g)}\right)\delta_u\right]\left(\sum_{k=1}^{i_m}F_k h_k + h_{i_m}\sum_{k=i_m+1}^{n_s}F_k\right) \end{aligned} \tag{12}$$

for type-1 mechanism;

$$\sum_{i=1}^{n_c} M_{c.ii_m}^{(2.1)} \ge \left[\gamma_{Rd}2M_{fl.Cd.n_s}\left(\frac{\sum_{k=1}^{n_s}\beta_k}{\sum_{k=1}^{n_s}F_k h_k} - \frac{\sum_{k=i_m}^{n_s}\beta_k}{\sum_{k=i_m}^{n_s}F_k\left(h_k - h_{i_m-1}\right)}\right) + \left(\gamma_{i_m}^{(2)} - \gamma^{(g)}\right)\delta_u\right]\sum_{k=1}^{i_m}F_k\left(h_k - h_{i_m-1}\right) \tag{13}$$

for type-2 mechanism;

$$\sum_{i=1}^{n_c} M_{c.ii_m}^{(3)} \ge \left[\gamma_{Rd}2M_{fl.Cd.n_s}\frac{\sum_{k=1}^{n_s}\beta_k}{\sum_{k=1}^{n_s}F_k h_k} + \left(\gamma_1^{(3)} - \gamma^{(g)}\right)\delta_u\right]\frac{\left(h_{i_m} - h_{i_m-1}\right)}{2}\sum_{k=i_m}^{n_s}F_k \tag{14}$$

for type-3 mechanism.

While for the $i_m = 1$ storey the design condition is only one Eq. (12) for the i_m>1 storeys, the sum of the reduced plastic moments of columns has to be calculated as the maximum among the three mechanism typologies, according to the following relation:

$$\sum_{i=1}^{n_c} M_{c.ii_m} = max\left\{\sum_{i=1}^{n_c} M_{c.ii_m}^{(1)}, \sum_{i=1}^{n_c} M_{c.ii_m}^{(2)}, \sum_{i=1}^{n_c} M_{c.ii_m}^{(3)}\right\} \tag{15}$$

The knowledge of these plastic moments, coupled with the estimated axial force at the collapse state, allows the evaluation of the required sections of columns.

The sum provided by Eq. (15) has to be distributed between all the columns at each storey according to two possible strategies [13]:

1) the sum are subdivided equally between each column

2) the sum are subdivided according to the axial load acting on the columns in the collapse condition.

However, in both the cases column sections need to verify the combination of the competent axial load at collapse and bending moment.

The axial load acting on the columns at collapse state can be easily provided in agreement with the global mechanism where axial forces in the columns at collapse state depend both on distributed loads acting on the beams and on the maximum axial load belonging to diagonal members [14], [27]. Also in this case, devices overstrength has to be taken in account according to the second capacity design principle. However, seismic actions can be acting either in the positive direction or in the negative direction, so that the maximum axial forces has to be considered.

3 WORKED EXAMPLE

Aiming to practically show how to apply the proposed design procedure a 3 bays 4 storeys pin-jointed column bases EBF whose structural scheme is depicted in Figure 3 has been designed. The bay span is 5 m while the interstorey height is equal to 3.0 m. The characteristic values of the vertical loads acting on beams are equal to $3{,}34 kN/m^2$ and $2{,}50\ kN/m^2$ for permanent and live loads, respectively, while on columns concentrated loads belonging to the secondary warping of floor are applied (Figure 3). With reference to the seismic load combination $(\mathrm{G_k} + \psi_2 \mathrm{Q_k} + \mathrm{E_d})$, the vertical loads acting on the beams of the analysed structure are $4{,}067\ kN/m$. The structural material adopted for all the structural members is an S275. The design horizontal forces have been determined according to EC8, assuming a peak ground acceleration equal to 0.35g, a seismic response factor equal to 2.5, a behaviour factor equal to 6. The design horizontal forces distribution is in accord to the first vibration mode as reported in Figure 3. In addition, vertical loads acting on the inner pendular structure are accounted for by means of a leaning column.

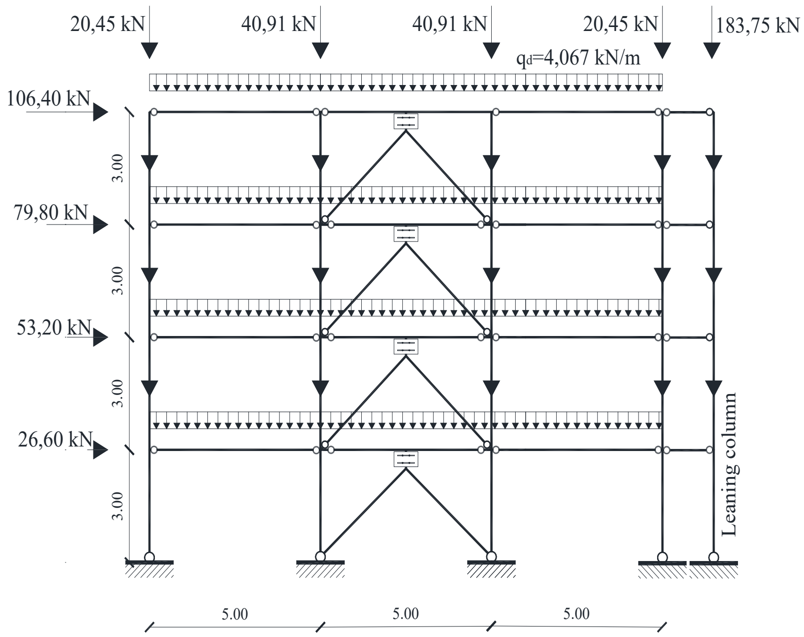

Figure 3: Worked example structural scheme

Frictional devices are made of a layer of friction material, placed between two bolted steel plates which accommodate an inner plate containing slotted holes that allow the slippage of the device. In addition, external plates have slotted holes also in vertical direction to allow vertical displacement due to vertical loads (Figure 4). Adopted bolts are high resistance class 8.8 while the friction material adopted (FREEDAM project) is sprayed aluminum that is able to exhibit a friction coefficient of about 0.5 [38]-[39].

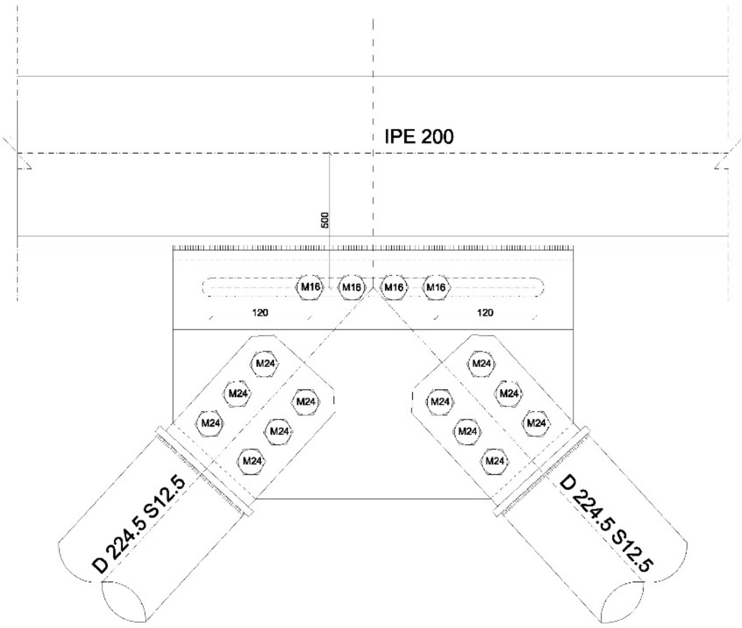

Figure 4: Scheme of dissipative device

3.1 Design of dissipative zones

The first quantity needed for the design of the structure is the design slip moment of devices at the last storey (storey n_s) provided by Eq. (4), being preliminarily compute the term $\sum_{k=1}^{n_s} \beta_k = 7{,}5$. Successively, the sum of the design slip moment $M_{fb.Ed.n_s}$ has to be shared between all the storeys by means of the term β_k to design the dissipative device preliminarily described, according to the following relation:

$$M_{fl.Ed.n_s} = n_s\, n_b\, N_b\, \mu\, e/2 \rightarrow M_{fl.Cd.n_s} \tag{16}$$

where, n_s is the number of frictional surfaces that in this case is equal to 2, n_b is number of bolts, N_b is the preloading force equal to:

$$N_b = 0.7\, f_{ub} A_s \tag{17}$$

f_{ub} is the design bolt resistance, A_s is the bolt area, μ is the dynamic frictional coefficient assumed in this case equal to 0.5 and e is the distance between the median axis of the beam and the intersection of brace axes assumed, in this case, equal to 0,5 m. In addition, beams are preliminarily selected from the standard shapes to withstand the vertical load combination $(1.3\mathrm{G_k} + 1.5Q_k)$ according to a design moment computed as in Eq. (6) and are IPE200. In Table 2 the sum of the design slip moment $M_{fl.Ed.k}$ shared at all the storey by means of the term β_k, the slip resistant moment $M_{fl.Cd.k}$, belonging to the device design, the number of bolts n_b, the distance e, the preloading force N_b are reported.

Storey (-)	β_k (-)	$M_{fb.Ed.k}$ $(kN\ m)$	n_b (-)	e (m)	Bolts (-)	N_b kN	$M_{fl.Cd.k}$ $(kN\ m)$	$\gamma_{Rd} M_{fl.Cd.k}\cdot$ $(kN\ m)$
	2.5	66.50	4	0.5	ϕ16	84.00	67.20	80.64
2	2.25	59.85	4	0.5	ϕ16	75.00	60.00	72.00
3	1.75	46.55	4	0.5	ϕ16	59.00	47.20	56.64
4	1	26.60	4	0.5	ϕ16	35.00	28.00	33.60

Table 2: Parameters for the design of beam-to-column connections

Finally, beam sections designed to withstand vertical loads have also to fulfil also the local hierarchy criterion reported in the second term of Eq. (6). Diagonal braces, designed to support in and out of plane buckling are D244,5 s12,5 tubes.

3.2 Design of non-dissipative zones

Being designed dissipative zones, also non-dissipative one have to be provided by means of TPMC. The ultimate design displacement governing the procedure has been computed in the following way:

$$\delta_u = 0.04\, h_{n_s} = 0.04 \cdot 12 = 0.48\, m \tag{18}$$

being assumed an ultimate device rotation equal to 0.04 and as a consequence a maximum device stroke of 0,12 m. In addition, in Table 3 the slopes of mechanism equilibrium curves are reported being computed according to the relationships reported in Table 1.

STOREY $\boldsymbol{i_m}$	$\boldsymbol{\gamma_{i_m}^{(1)}}$ (1/m)	$\boldsymbol{\gamma_{i_m}^{(2)}}$ (1/m)	$\boldsymbol{\gamma_{i_m}^{(3)}}$ (1/m)
1	0.308	<u>0.064</u>	0.308
2	0.142	0.077	0.256
3	0.089	0.105	0.220
4	0.064	0.192	0.192

Table 3. Slopes of the mechanism equilibrium curves

It is possible to observe that the slope of the global mechanism equilibrium curve (undersigned in Table 3) is the minimum among all the slope of mechanism equilibrium curves corresponding to the undesired mechanism. In addition, in Table 4 the design bending moment of columns at each storey are reported.

STOREY $\boldsymbol{i_m}$	$\boldsymbol{\sum_{i=1}^{n_c} M_{c.ii_m}^{(1)}}$ (kN m)	$\boldsymbol{\sum_{i=1}^{n_c} M_{c.ii_m}^{(2)}}$(kN m)	$\boldsymbol{\sum_{i=1}^{n_c} M_{c.ii_m}^{(3)}}$(kN m)	$\boldsymbol{\sum_{i=1}^{n_c} M_{c.ii_m}}$(kN m)
1	841.741	[-]	841.741	841.741
2	521.3593	84.3591	302.8592	521.3593
3	235.0923	140.1408	187.6165	235.0923
4	[-]	161.8078	80.9039	161.8078

Table 4. Value of the paramters $\sum_{i=1}^{n_c} M_{c.ii_m}^{(t)}$

In this worked example the approach that have been used to subdivide the reduced sum of plastic moments between the columns exploits the axial load acting on the columns at collapse state. In fact, the maximum value of $M_{c,i_m}$is subdivided between columns on the basis of axial force acting on each column at each storey.

The reduced sum of plastic moments of columns at each storey, $\sum_{i=1}^{n_c} M_{c.ii_m}$, has been subdivided proportionally to the axial load at the collapse state according to the following equation:

$$M_{c.ik} = \frac{N_{tot.ii_m} \sum_{i=1}^{n_c} M_{c.ii_m}}{\sum_{i=1}^{n_c} N_{tot.ii_m}} \tag{19}$$

where $M_{c.ik}$ is the design moment of column sections.

Finally, in Table 5 the axial load acting at the collapse state, the design moment of column sections and the column sections selected from standard shapes are reported with reference to external and internal columns. The collapse mechanism multiplier of global mechanism α is equal to 1.2175.

STOREY i_m	External columns			Internal columns		
	$N_{tot.ii_m}$ (kN)	$M_{c.ik}$ (kN m)	PROFILES	$N_{tot.ii_m}$ (kN)	$M_{c.ik}$ (kN m)	PROFILES
1	122.50	74.50	HE 160 B	569.48	346.36	HE 280 B
2	91.87	52.51	HE 140 B	364.23	208.17	HE 220 B
3	61.25	28.70	HE 120 B	189.70	88.86	HE 160 B
4	30.62	26.97	HE 100 B	61.25	53.93	HE 140 B

Table 5. Axial force at collapse state, design moment of column sections and column sections selected from standard shapes at each storey

4 VALIDATION OF PROCEDURE

In order to validate the design procedure static non linear analysis (push-over) has been carried out for the designed EBF frame by means of SAP 2000 computer program [44]. This analysis has the primary aim to predict the collapse mechanism typology, testing the accuracy of the proposed design methodology.

In SAP2000 ambiance all members have been modeled by means of beam-column elements, whose non-linearities have been concentrated in plastic hinges at their ends. In particular, plastic hinges accounting for the interaction between axial force and bending moment have been defined for, columns while dissipative devices have been modelled in shear-elongation such as short links [40]-[43]. Beams and diagonals have been modelled with pure bending plastic hinges and force bending, respectively. The elastic behaviour is not considered in plastic hinge definition because it is directly taken into account by the beam-column element. The analysis has been led under displacement control taking into account both geometrical and mechanical non-linearities. In addition out of plan stability check of compressed members have been performed at each step of the non-linear analysis. The results of the push-over are mainly constituted by the frame capacity curve (Figure 4) whose softening branch is perfectly coincident to the global mechanism equilibrium curve. In addition, push-over curve show a very pronounced elbow that is symptomatic of a contemporary activation of all the dissipative devices and of a consequent seismic energy optimization in terms of dissipative capacity of the structure.

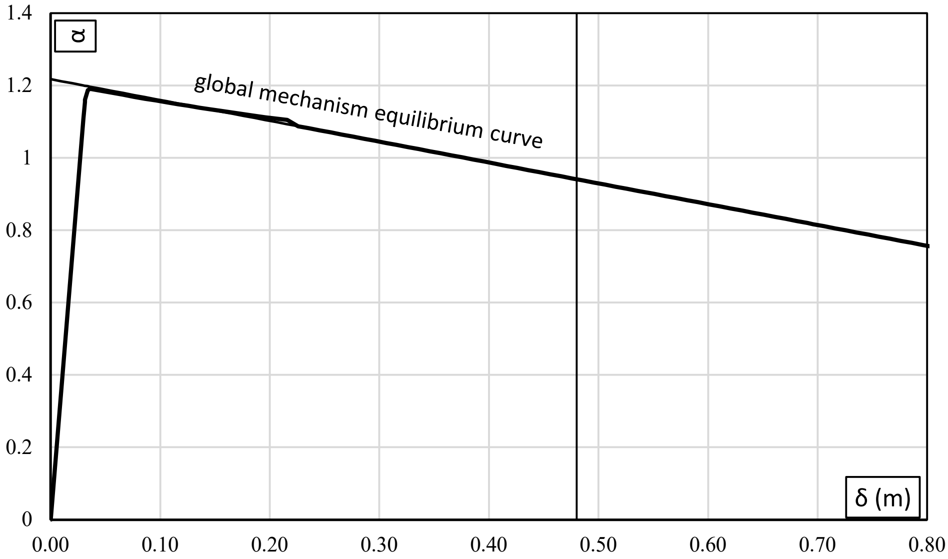

Figure 5: Push-over curve of the analyzed structure

In addition, in order to provide a more robust validation of the design methodology, non-linear incremental dynamic analyses have been carried out with reference to the same structural model used for push-over analyses. In addition, 5% damping according to Rayleigh modelling has been assumed.

Record-to-record variability has been accounted for considering 10 recorded accelerograms selected from PEER [45] data base whose main characteristics (name, date, magnitude, ratio between PGA and gravity acceleration, length and step recording) are reported in Table 6. These earthquake records have been selected to approximately match the linear elastic design response spectrum of Eurocode 8 [4], for type A soil (Figure 6). Moreover, in order to perform IDA analyses, each ground motion has been scaled to obtain the same value of the spectral acceleration Sa (T_1) corresponding to the fundamental period of vibration T_1 of the structure (T_1=0,785 s). This is the seismic intensity measure (IM) adopted for IDA analyses where Sa(T_1) values have been progressively increased until the occurrence of structural collapse, corresponding to anyone of the following ultimate limit states: column buckling, complete development of a collapse mechanism, attainment of the limit value of the devices stroke.

Earhquake (record)	Component	Date	PGA/g	Length (s)	Step recording (s)
Coalinga (Slack Canyon)	H-SCN045	1985/05/02	0.166	29.99	0.01
Helena (Carroll College)	A-HMC180	1976/09/15	0.150	39.99	0.01
Imperial Valley (Agrarias)	H-AGR003	1979/10/15	0.370	28.35	0.01
Kobe (Kakogawa)	KAK000	1995/01/16	0.251	40.95	0.01
Northridge (Stone Canyon)	SCR000	1994/01/17	0.252	39.99	0.01
Santa Barbara (Courthouse)	SBA132	1978/08/13	0.102	12.57	0.01
Spitak Armenia (Gaukasian)	GKS000	1998/12/07	0.199	19.89	0.01
Friuli, Italy (Tolmezzo)	TMZ000	1976/05/06	0.351	36.345	0.005
Irpinia (Calitri)	A-CTR000	1980/11/23	0.132	35.79	0.0024
Victoria, Mexico (Chihuahua)	CHI102	1980/06/09	0.150	26.91	0.01

Table 6: Accelerogram characteristics

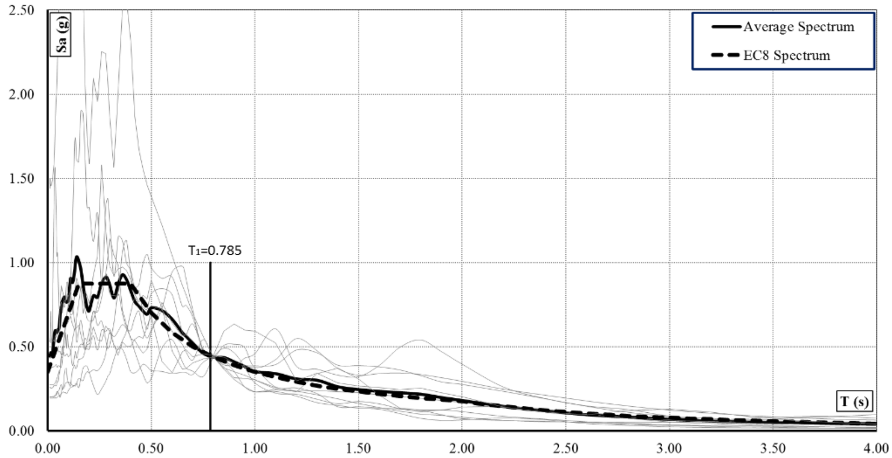

Figure 6: Response spectra (soil type A, ζ=5%) scale at the same value of Sa for T1=0,785

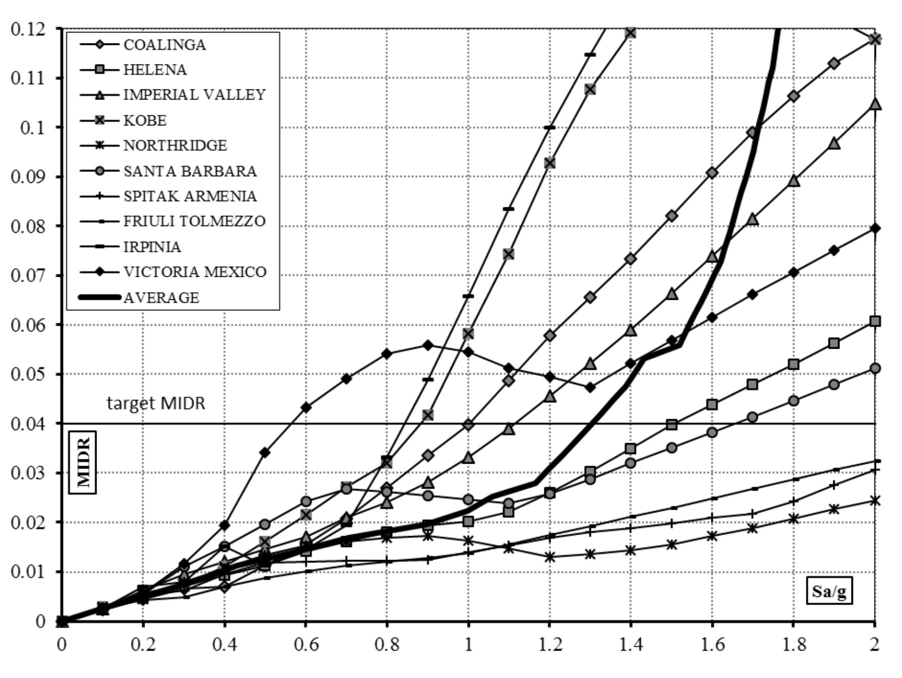

Figure 7: Maximum Interstorey Drift Ratio (MIDR) vs Spectral Acceleration (Sa/g)

In Figure 6 the Maximum Interstorey Drift Ratio vs Spectral Acceleration is reported. MIDR curves appears regular and quite always increasing reaching on average a spectral acceleration of 1,30 g corresponding to the achievement of the target drift equal to 0.04 rad. In addition, for each accelerogram, the obtained pattern of yielding has been monitored as far as the spectral acceleration increases confirming the development of a global mechanism.

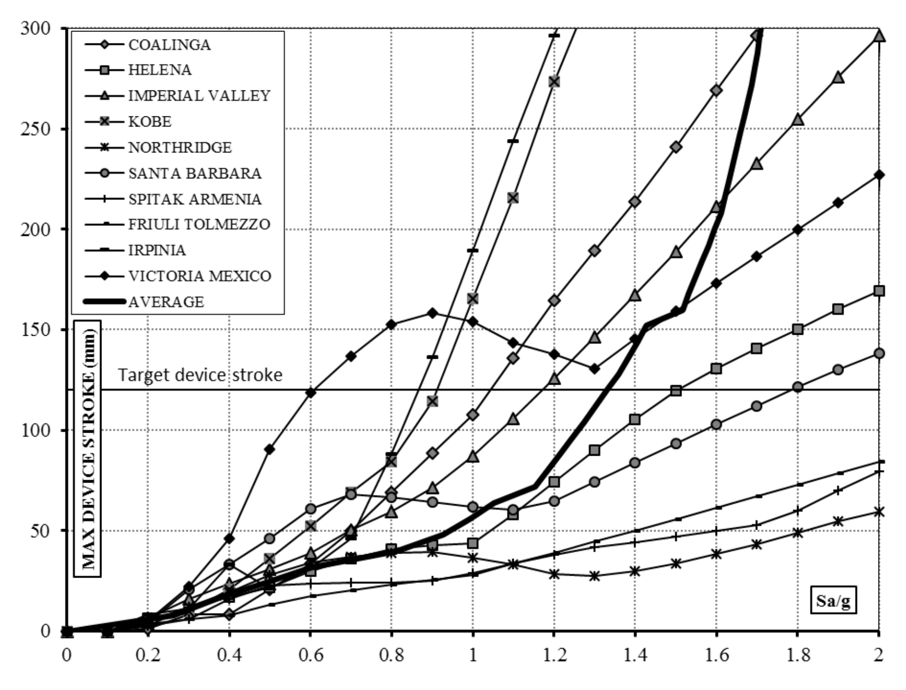

Figure 8: Maximum Device Stroke vs Spectral Acceleration (Sa/g)

Finally, in Figure 7 the maximum device stroke versus the spectral acceleration is reported. In particular, a spectral acceleration of 1.23g is achieved on average also for a target stroke of 0,12 m. This result is in perfect agreement with those deduced by the MIDR graph. This high values of spectral acceleration are very satisfactory and confirms the high dissipative performances of EBFs especially if equipped with dissipative friction devices.

5 CONCLUSIONS

- In this work EBFs equipped with frictional devices have been analyzed.
- The control of devices activation and, as a consequence, the optimization of energy dissipation capacity is obtained by a rigorous design procedure assuring that only the dissipative zones are involved in plastic range while non dissipative ones remain elastic called theory of Plastic Mechanism Control.
- Being all the non dissipative zones in elastic range and only frictional devices activated in plastic range the structure can be considered as free from damage. In fact, after a destructive seismic event all the damaged devices can be replaced by new ones.
- In addition, by designing dissipative zones proportionally to the storey shear they are assured to be engaged in yielding as contemporary as possible, benefit optimization of the seismic response.
- The accuracy of the design approach has been investigated by means push-over and nonlinear dynamic analyses by applying a properly chosen set of earthquake ground motions.
- The global mechanism is confirmed to be achieved by both push-over than IDA Analyses.
- The designed structure show very high performances due both to the accuracy of the design procedure than to the exploitation of dissipative capacity of devices.

REFERENCES

[1] Kasai K, Popov E.P.: "General behavior of WF steel shear link beams", ASCE Journal of Structural Engineering, Vol. 112, Issue 2, pp. 362-382, 1986.

[2] Kasai K., Han X.: "New EBF design method and applications: Redesign and analysis of US-Japan EBF. Proceedings of Stessa 97 – 2nd international conference on behaviour of steel structures in seismi areas, 1997.

[3] Kasai K., Han X.: "Refined Design and Analysis of Eccentrically Braced Frames", Journal of Structural Engineering, ASCE, 1997.

[4] EN 1998-1: "Eurocode 8: Design of Structures for Earthquake Resistance – Part 1: general Rules, Seismic Actions and Rules for Buildings", CEN, 2004

[5] Castaldo P, Palazzo B, Della Vecchia P., "Seismic reliability of base-isolated structures with friction pendulum bearings", *Engineering Structures*, Vol. 95, 80-93, 2015

[6] Castaldo P, Tubaldi E., "Influence of FPS bearing properties on the seismic performance of base-isolated structures", *Earthquake Engineering and Structural Dynamics* 2015; Vol. 44, 2817–2836, 2015.

[7] Castaldo P., "Integrated Seismic Design of Structure and Control Systems", *Springer International Publishing: New York*, 2014. DOI 10.1007/978-3-319-02615-2, 2014.

[8] Castaldo P., De Iuliis M., "Optimal integrated seismic design of structural and viscoelastic bracing-damper systems", *Earthquake Engineering and Structural Dynamics*, Vol. 43(12),1809–1827, 2014.

[9] De Iuliis M., Castaldo P., "An energy-based approach to the seismic control of one-way asymmetrical structural systems using semi-active devices", *Ingegneria Sismica - International Journal of Earthquake Engineering 2012*; XXIX(4):31–42, 2012.

[10] Palazzo B, Castaldo P, Marino I. The Dissipative Column: A New Hysteretic Damper. Buildings 2015;5(1):163-178;

[11] Montuori R., Nastri E., Piluso V. Theory of plastic mechanism control for the seismic design of braced frames equipped with friction dampers - *Research Communications* – Vol. 58. pp. 112-123 2014.

[12] Mazzolani, F.M., Piluso, V., "Plastic Design of Seismic Resistant Steel Frames", Earthquake Engineering and Structural Dynamics, Vol. 26, pp. 167-191, 1997.

[13] Montuori, R., Nastri, E., Piluso, V., "Advances in Theory of Plastic Mechanism Control: Closed Form Solution for Mr-Frames", *Earthquake Engineering and Structural Dynamics*, 2015.

[14] Montuori, R., Nastri, E., Piluso, V., "Theory of plastic mechanism control for MRF-EBF dual systems: Closed Form Solution", Submitted for publication to Engineering Structures, 2016.

[15] Longo, A.; Montuori, R.; Piluso, V. Theory of Plastic Mechanism Control for MRF-CBF dual system and its validation. *Bulletin of Earthquake Engineering* (BEEE). 2014.

[16] Giugliano M.T., Longo A., Montuori R., Piluso V. Failure mode and drift control of MRF-CBF dual systems *The Open Construction and Building Technology Journal*, 4, 121-133, 2010.

[17] Montuori R., Piluso V., Troisi M. Theory of plastic mechanism control of seismic-resistant MR-frames with set-backs. *Open Construction and Building Technology Journal*, vol. 6, pp. 404-413 , 2012.

[18] Longo A., Montuori R., Piluso V., Theory of Plastic Mechanism Control of Dissipative Truss Moment Frames, *Engineering Structures*, Vol. 37, pp. 63-75, 2012.

[19] Longo A., Montuori R., Piluso V., Failure Mode Control and Seismic Response of Dissipative Truss Moment Frames, *Journal of Structural Engineering*, Vol. 138, pp.1388-1397, 2012.

[20] Longo A., Montuori, R., Nastri, E., Piluso, V. On the use of HSS in seismic-resistant structures *Journal of Constructional Steel Research*, Vol. 103, p. 1-12, 2014.

[21] Longo A., Montuori, R., Piluso, V., Moment Frames - Concentrically Braced Frames Dual Systems: Analysis of Different Design Criteria, *Structure and infrastructure engineering*, Volume 12, Issue 1, 2 January 2016, Pages 122-14.

[22] Longo A., Nastri E., Piluso V. Theory of plastic mechanism control: State-of-the-art. Open Construction and Building Technology Journal. Volume 8, 2014, Pages 262-278

[23] Longo A., Montuori R., Piluso V. Failure mode control of X-braced frames under seismic actions. *Journal of Earthquake Engineering*, 12: 728-759, 2008

[24] Longo A, Montuori R, Piluso V. Plastic design of seismic resistant V-Braced frames. *Journal of Earthquake Engineering,* vol. 12: 1246-1266, 2008.

[25] Longo A, Montuori R, Piluso V. "Influence of design Criteria on the seismic Reliability of X-Braced Frames", *Journal of Earthquake Engineering*, Vol. 12, Issue 3– p.406-431. 2008

[26] Montuori, R., Nastri, E., Piluso, V.,"Rigid-plastic analysis and moment–shear interaction for hierarchy criteria of inverted Y EB-Frames" *Journal of Constructional Steel Research* vol. 95 71-80. 2014.

[27] Montuori, R., Nastri, E., Piluso, V., Theory of Plastic Mechanism Control for Eccentrically Braced Frames with inverted Y-scheme, *Journal of Constructional Steel Research*, Volume 92, pp. 122-135, 2014.

[28] Giugliano M.T., Longo A., Montuori R., Piluso V., Plastic design of CB-frames with reduced section solution for bracing members. *Journal of Constructional Steel Research.* Vol. 66 pp 611-621. 2010.

[29] Longo A., Montuori R., Piluso V. Seismic reliability of V-braced frames: Influence of design methodologies. *Earthquake Engineering and Structural Dynamics*, vol. 38 p. 1587-1608, 2009.

[30] Longo A., Montuori R., Piluso V. Seismic Reliability of Chevron Braced Frames with Innovative Conception of Bracing Members, *Advanced Steel Construction, an International Journal* - Vol. 5, No. 4, December 2009.

[31] Montuori, R. , Muscati, R. Plastic design of seismic resistant reinforced concrete frame. Earthquake and Structures Volume 8, Issue 1, 2015, Pages 205-224.

[32] Montuori, R. , Muscati, R. A General Procedure for Failure Mechanism Control of Reinforced Concrete Frames. Submitted for publication to Engineering Structures.

[33] Ohsaki M., Nakajima T.: "Optimization of Link Member of Eccentrically Braced Frames for Maximum Energy Dissipation", Journal of Constructional Steel Research, Vol. 75, 2012, pp. 38-44, 2012.

[34] Latour, M., Piluso, V., Rizzano, G. Free from damage beam-to-column joints: Testing and design of DST connections with friction pads. Engineering Structures. Volume 85, February 05, Pages 219-233, 2015.

[35] Montuori R., Piluso V., Troisi M. Innovative structural details in MR-frames for free from damage structures Mechanics Research Communications – Vol. 58 pp. 146-156. 2014.

[36] Lee S-S., Goel S.C., "Performance-Based Design of Steel Moment Frames using Target Drift and Yield Mechanism", Research Report UMCEE 01-17, University of Michigan, December 2011.

[37] Goel S.C., Chao S-H., "Performance-Based Plastic Design: Earthquake Resistant steel Structures", International Code Council: Washington, DC, 2008.

[38] Latour M., Rizzano G., Piluso V. (2012): "Experimental Analysis of Innovative Dissipative Bolted Double Split Tee Beam-to-Column Connections", *Steel Construction*, 4 (2011), N.2, 53-64.

[39] Latour M., Piluso V., Rizzano G. (2014), "Experimental analysis on friction materials for supplemental damping devices", Construction and Building Materials, Volume 65, 29 August 2014, 159-176.

[40] Della Corte G., D'Aniello M., Landolfo R., (2013). Analytical and numerical study of plastic overstrength of shear links. Journal of Constructional Steel Research, 82, 19–32

[41] Della Corte G., D'Aniello M., Mazzolani F.M., "Inelastic response of shear links with axial restraints: numerical vs. analytical results" 5th International Conference on Advances in Steel Structures, Singapore, 5 – 7 December, 2007.

[42] Mastandrea L., Nastri E., Piluso, V., "Validation of a Design Procedure for Failure Mode Control of EB-Frames: Push-over and IDA analyses", The Open Construction and Building Technology Journal, 7, 193-207, 2013.

[43] Bosco, M., Marino, E.M., Rossi, P.P., "Modelling of steel link beams of short, intermediate or long length", Engineering Structures, Volume 84, February 01, Pages 406-418, 2015.

[44] CSI 2007. SAP 2000: Integrated Finite Element Analysis and Design of Structures. Analysis Reference. Computer and Structure Inc. University of California, Berkeley.

[45] Pacific Earthquake Engineering Research Center, PEER Strong Motion Database, http://peer.berkley.edu.smcat.